THE ASTROPHYSICAL JOURNAL, 395:192–201, 1992 August 10

AN RR LYRAE PERIOD SHIFT IN TERMS OF THE FOURIER PARAMETER ϕ_{31}

CHRISTINE M. CLEMENT AND MICHAEL JANKULAK
David Dunlap Observatory, Department of Astronomy, University of Toronto, Toronto, Ontario, Canada, M5S 1A1
AND
NORMAN R. SIMON
Department of Physics and Astronomy, University of Nebraska, Lincoln, NE 68588
Received 1991 November 14; accepted 1992 February 18

ABSTRACT

The Fourier phase parameter ϕ_{31} has been determined for RR*c* stars in five globular clusters, NGC 6171, M5, M3, M53, and M15. The results indicate that the RR*c* stars in a given cluster show a sequence of ϕ_{31} increasing with period, and that the higher the cluster metallicity, the higher the sequence lies in a plot of ϕ_{31} with period. The ϕ_{31} values for the stars in NGC 6171 and M5 presented here are based on observations made with the University of Toronto 0.61 m telescope at Las Campanas, Chile, while those for M3, M53, and M15 are based on published data. A bootstrap procedure has been used to establish the uncertainties in the Fourier parameters. The physical significance of the relationship among ϕ_{31}, period, and metallicity is not yet understood. It will need to be tested with hydrodynamic pulsation models computed with new opacities.

Subject headings: globular clusters: general — stars: oscillation — stars: variables: others

1. INTRODUCTION

The RR Lyrae variables comprise a subject which is both important and vigorously debated. These stars could play a crucial role in the study of galactic structure and the cosmic distance scale, but their masses and luminosities remain uncertain. Mass determinations employing the RR*d* stars, always controversial, have now been thrown into turmoil with the advent of new opacities (Iglesias & Rogers 1991) which make the inferred RR*d* masses highly dependent on metallicity (Cox 1991). The canonical RR*d* mass segregation of Oosterhoff I and II clusters might now be erased (or even reversed!), subject to precise determinations of cluster element abundances (Kovács, Buchler, & Marom 1991).

Meanwhile, calculation of horizontal branch (HB) evolution, which could also supply RR Lyrae masses and luminosities, have struggled with the problem of the "period-shift effect." This refers to the increase in cluster RR Lyrae periods (at given temperature) with decreasing metallicity of the cluster (Sandage 1982). To date, HB evolutionary tracks have failed to reproduce the period shift without making unpalatable assumptions (Rood 1990; Simon 1992; but for a contrary view, see Lee, Demarque, & Zinn 1990). However, the period-shift effect, or at least its magnitude, has itself been called into question (e.g., Lee et al. 1990), principally due to the difficulty in accurately measuring RR Lyrae temperatures. Rood (1990) concludes that the observational basis for the Sandage period shift lies primarily in the comparison of two particular clusters, M3 and M15.

Yet another potential method for determining masses and luminosities of RR Lyrae stars employs the structural characteristics of the observed light curves. These are obtained by the technique of Fourier decomposition (Simon 1988), wherein the observed magnitudes are fitted with a Fourier series

$$\text{mag} = A_0 + \sum_{j=1,n} A_j \cos(j\omega t + \phi_j), \quad (1)$$

and the shape of the light curve quantified in terms of the lower order coefficients, viz., $R_{j1} = A_j/A_1$, $\phi_{j1} = \phi_j - j\phi_1$ ($j = 1, 2, 3, 4$). Peterson (1984) applied this technique to observations (Martin 1938) of the RR Lyraes stars in the globular cluster ω Centauri, finding among the RR*c* stars a definite trend of increase of the Fourier phase parameter ϕ_{31} with period. Later, Simon (1989, 1990) showed that standard hydrodynamic pulsation models were able to reproduce this trend, and he attributed the observed spread in ϕ_{31} at a given period to a spread in mass among the ω Centauri RR*c* stars. Guided by the canonical RR*d* mass segregation (now called into question; see above), Simon predicted that OoI (e.g., M3) and OoII (e.g., M15) cluster RR*c* stars should be separated on the ϕ_{31} versus period diagram, with the former lying above the latter. However, because the measurement of ϕ_{31} places considerable demands on the observations, the testing of this prediction has so far been frustrated.

In this paper we describe new observations for RR*c* stars in two clusters, NGC 6171 and M5, and use these along with existing data for a number of other clusters (M3, M15, and M53) to display the ϕ_{31} versus period diagram as a function of metallicity. All of the clusters are seen to show the trend of increase of ϕ_{31} with period. Furthermore, we find that the lower the metallicity of the cluster, the longer the RR*c* period at fixed ϕ_{31}. This appears to be the Sandage period shift in another guise.

2. THE OBSERVATIONAL DATA

The University of Toronto 0.61 m f/15 Cassegrain telescope at the Las Campanas Observatory of the Carnegie Institution of Washington was used from 1972 to 1991 for a photographic study of the globular clusters NGC 6171 and Messier 5 (NGC 5904). These observations were made for an investigation of the long-term behavior of the periods of the RR Lyrae stars, but it appears that they may provide appropriate data for Fourier analysis as well. At the present time, not all of the observations have been reduced. However, a substantial number of plates of each cluster have been measured, and *B*-magnitudes have been determined for most of the RR Lyrae variables. The actual magnitudes are not tabulated in this

paper, but will be published in the future, as part of the study of the long-term behavior of the RR Lyrae variables in these two clusters.

The two clusters are interesting to examine because, although they are both relatively metal rich, they have different metal abundances, with [Fe/H] = −0.99 for NGC 6171 and −1.40 for M5, according to Suntzeff, Kinman, & Kraft (1991). Fourier decomposition parameters for the RR*c* stars in NGC 6171, based on photographic observations by Dickens (1970), have already been published by Kovács, Shlosman, & Buchler (1986) and by Stellingwerf & Dickens (1987), but neither of these studies gives any evidence for a systematic increase of ϕ_{31} with period, similar to the trend observed in ω Centauri by Petersen (1984). However, since the number of observations available in the Dickens data was quite limited—45 *V* plates, 48 *B* plates and 25 *U* plates—one cannot rule out the possibility of a ϕ_{31}–period relationship. It is therefore worthwhile to analyze the more extensive data from Las Campanas because the phase coverage is better.

In addition to the photometry of NGC 6171 and M5, extensive Las Campanas observations have also been made of ω Centauri. While these observations have not yet undergone systematic treatment, a special effort was made to analyze the pulsations of a few RR*c* stars, in order to compare the results with those of Petersen (1984). These comparisons are described in the next section in connection with a discussion of uncertainties in the Fourier decomposition parameters. The bulk of the Las Campanas ω Centauri data will be published and discussed at a later time.

3. THE ANALYSIS OF THE LAS CAMPANAS OBSERVATIONS

3.1. *ω Centauri*

Petersen (1984) published Fourier parameters for 20 RR*c* and 20 RR*ab* variables in ω Centauri. Of these stars, 8 *RRc* (V16, V19, V64, V76, V82, V83, V105, and V127) and 9 RR*ab* (V5, V8, V9, V23, V51, V56, V67, V74, and V113) variables have been measured on the Las Campanas plates. To compare the parameters derived from the two data sets, we analyzed the 157 observations made in the interval 1977–1981. Three RR*c* stars (V19, V105, and V127) and one RR*ab* star (V5) were selected to give a reasonable representation of the Las Campanas data. Among the RR*c* stars, the light curve of V19 showed the least amount of scatter, that of V127 the most, and the quality of the light curve for V105 was average. The light curve for V5 showed an average amount of scatter for an RR*ab* star. The reason for the excessive scatter in the light curve of V127 was that this star was located near the edge of the field on the Las Campanas plates. One would expect that such a star would not be a suitable candidate for Fourier analysis, but it is an interesting experiment to carry out the analysis to see the results.

For each data set and each of the four stars, we determined the Fourier decomposition parameters by fitting equation (1) to the observations. In each case, the epoch was taken as JD 2400000.000 so that t in equation (1) refers to (JD −2400000.000), where JD represents the Julian date of the observation. For each star, the period was determined using a program based on Stellingwerf's (1978) phase dispersion minimization (PDM) technique. If the PDM period gave a better fit to the observations than the published period, the former was used for the Fourier analysis. Peterson (1984) tabulated average values for the amplitude ratios, R_{21}, R_{31}, and R_{41}, and phase differences, ϕ_{21}, ϕ_{31}, and ϕ_{41}, based on fits for orders $n = 4$, 5, 6, and 7 to Martin's mean points. In order to compare our data with his, we calculated the same parameters using Martin's actual observations and the Las Campanas observations. The results are shown in Table 1. The parameters calculated for the RR*ab* star, V5, for the two data sets agree very well. This is apparently due to the fact that the amplitudes are larger for RR*ab* stars, and thus, both the phases and amplitudes can be determined with greater precision, than for the RR*c* stars. It should be noted that the magnitude calibrations for the two sets of observations are different. Martin's observations were made with blue-sensitive photographic emulsions and no filter. He calibrated the magnitudes for his sequence stars by using the Mount Wilson Catalogue of Selected Areas (Seares et al. 1930). The Las Campanas observations were made with 103aO photographic emulsion through a GG385 filter to give magnitudes on the *B* system. The *B*-magnitudes for the standard sequence were taken from the photographic data published in Royal Observatory Annals, Number 2 (Woolley 1966). Even though the magnitude calibrations are different, the amplitude ratios appear to be similar. The parameters for the RR*c* stars do not agree as well as those for V5, but we do find that the phase differences, ϕ_{21} and ϕ_{31} are in fairly good agreement. The important exceptions are in ϕ_{21} for V105 (where the Las Campanas observations give a different value

TABLE 1

COMPARISON OF FOURIER PARAMETERS—ω CENTAURI

Star	Source	P (days)	R_{21}	R_{31}	R_{41}	ϕ_{21}	ϕ_{31}	ϕ_{41}
V5	Martin's mean points	0.5153	0.438	0.295	0.235	3.91	1.67	5.87
	Martin's observations		0.435	0.300	0.240	3.91	1.70	5.88
	Las Campanas data		0.455	0.332	0.231	3.84	1.69	5.84
V19	Martin's mean points	0.2996	0.128	0.105	0.055	4.71	3.37	2.26
	Martin's observations		0.125	0.101	0.065	4.63	3.31	2.37
	Las Campanas data		0.152	0.049	0.075	5.12	3.48	2.06
V105	Martin's mean points	0.3353	0.054	0.087	0.025	5.47	4.14	3.04
	Martin's observations		0.058	0.082	0.032	5.45	4.24	3.05
	Las Campanas data		0.021	0.066	0.037	4.56	4.25	3.57
V127	Martin's mean points	0.3053	0.106	0.028	0.084	4.45	3.44	0.67
	Martin's observations		0.100	0.038	0.046	4.70	2.65	0.87
	Las Campanas data		0.178	0.096	0.038	4.50	2.66	2.67

NOTES.—The amplitude ratios (R_{j1}) and phase differences (ϕ_{j1}) are the mean values of orders $n = 4$, 5, 6, and 7.

from those of Martin) and in ϕ_{31} for V127 (for which Martin's mean points give a different value from those determined from the actual observations). Clearly, one needs to be able to assess the accuracy of these parameters.

3.2. *The Uncertainties of the Fourier Parameters*

To assess the uncertainties in the calculated values of the Fourier parameters, we have used Petersen's (1986) simple approximations for the standard errors and Efron's bootstrap procedure (Diaconis & Efron 1983). The bootstrap method is a means of estimating the statistical accuracy of a particular parameter from the data in a single sample. A number of "bootstrap" samples are generated from the original data, and the parameter of interest is calculated for each bootstrap sample. The distribution of the parameters thus calculated is treated as a distribution constructed from real samples. Some applications of the method to gamma-ray astronomy have been discussed by Simpson & Mayer-Hasselwander (1986).

Errors were estimated by both methods for the parameters of the four stars V5, V19, V105, and V127 in ω Centauri, for both sets of observations. For this analysis, the Fourier parameters were determined for order $n = 4$. The bootstrap procedure was applied in the following manner. For a star with N observations, a bootstrap sample was formed by taking N observational points selected at random from among all the observations, so that any one observation could occur no times, one time, or many times (Simpson & Mayer-Hasselwander 1986). The number of samples calculated in this manner for each star was 1000. For each sample, the N points were fitted with equation (1), and the Fourier phase differences and amplitude ratios were calculated. Table 2 gives the resulting frequency distributions of the Fourier phases, listing, for each star and data set, the intervals containing 68%, 90%, 95%, and 98% of the 1000 ϕ_{j1} values determined from the bootstrap samples. For example, the actual value of ϕ_{21} determined from the Las Campanas data for V5 is 3.86. When the bootstrap is applied, 68% of the 1000 samples yield ϕ_{21} values between 3.79 and 3.90, 90% between 3.76 and 3.93, etc. Figure 1 shows the histograms plotted for ϕ_{31} for the four stars (V5, V19, V105, and V127). Most of the histograms in Figure 1 resemble bell-shaped curves. However, Martin's data for V127 is an exception. The distribution for this star is distinctly bimodal. Apparently, this structure occurs because a substantial number of the observations are scattered off the light curve. To determine if this distribution would persist, we generated another 1000 bootstrap samples, and when they were plotted, the resulting histogram had the same form. In fact, the intervals containing 68%, 90%, 95%, and 98% of the ϕ_{31} values all agreed to within 0.02 with those listed in Table 2 for this star. Thus it appears that 1000 bootstrap samples are sufficient to establish the shape of the ϕ_{31} distribution.

Following Diaconis & Efron (1983), we shall employ as the bootstrap accuracy measure the width of the central interval containing 68% of the values. Half of this width will thus be interpreted as the average amount by which the calculated

TABLE 2

FREQUENCY DISTRIBUTION OF ϕ_{j1} FOR BOOTSTRAP SAMPLES OF SELECTED RR LYRAE VARIABLES IN ω CENTAURI

Star	Source	ϕ_{j1}	Distributions of the ϕ_{j1} values calculated from bootstrap samples			
		(real data)	68%	90%	95%	98%
V5–ϕ_{21}	Martin	3.92	3.87–3.95	3.84–3.96	3.82–3.97	3.81–3.98
	Las Campanas	3.86	3.79–3.90	3.76–3.93	3.74–3.94	3.71–3.96
ϕ_{31}	Martin	1.71	1.65–1.77	1.62–1.82	1.61–1.84	1.60–1.87
	Las Campanas	1.77	1.69–1.84	1.64–1.89	1.63–1.92	1.60–1.96
ϕ_{41}	Martin	6.07	5.97–6.11	5.93–6.14	5.91–6.16	5.90–6.18
	Las Campanas	5.91	5.75–6.02	5.68–6.12	5.65–6.17	5.60–6.21
V19–ϕ_{21}	Martin	4.62	4.48–4.71	4.42–4.76	4.39–4.78	4.37–4.80
	Las Campanas	5.03	4.83–5.16	4.74–5.25	4.70–5.31	4.65–5.35
ϕ_{31}	Martin	3.30	3.11–3.48	3.01–3.56	2.97–3.60	2.93–3.63
	Las Campanas	3.53	3.23–3.78	3.00–3.99	2.85–4.11	2.70–4.19
ϕ_{41}	Martin	2.41	2.15–2.64	2.02–2.75	1.98–2.80	1.92–2.90
	Las Campanas	2.10	1.75–2.37	1.42–2.58	1.08–2.73	0.70–2.98
V105–ϕ_{21}	Martin	5.45	5.03–5.60	4.77–5.70	4.62–5.74	4.44–5.79
	Las Campanas	4.54	3.36–5.36	2.28–6.17	1.74–6.54	1.32–6.96
ϕ_{31}	Martin	4.21	3.97–4.24	3.88–4.32	3.84–4.36	3.78–4.42
	Las Campanas	4.19	3.90–4.45	3.69–4.69	3.54–4.82	3.37–4.92
ϕ_{41}	Martin	3.04	2.46–3.61	2.14–3.86	1.92–3.96	1.78–4.06
	Las Campanas	3.40	1.83–4.47	0.69–5.74	0.31–6.07	0.10–6.16
V127–ϕ_{21}	Martin	4.73	4.60–4.88	4.52–4.98	4.48–5.02	4.44–5.08
	Las Campanas	4.52	4.19–4.82	3.97–5.00	3.84–5.09	3.62–5.21
ϕ_{31}	Martin	2.71	1.85–3.71	1.66–3.92	1.60–4.02	1.52–4.17
	Las Campanas	2.60	1.76–3.38	0.75–4.03	0.28–4.46	-0.10–4.98
ϕ_{41}	Martin	0.90	0.10–1.48	-0.46–1.80	-0.64–1.88	-0.86–2.01
	Las Campanas	2.54	0.43–3.44	-0.57–4.36	-0.82–4.70	-0.98–4.86

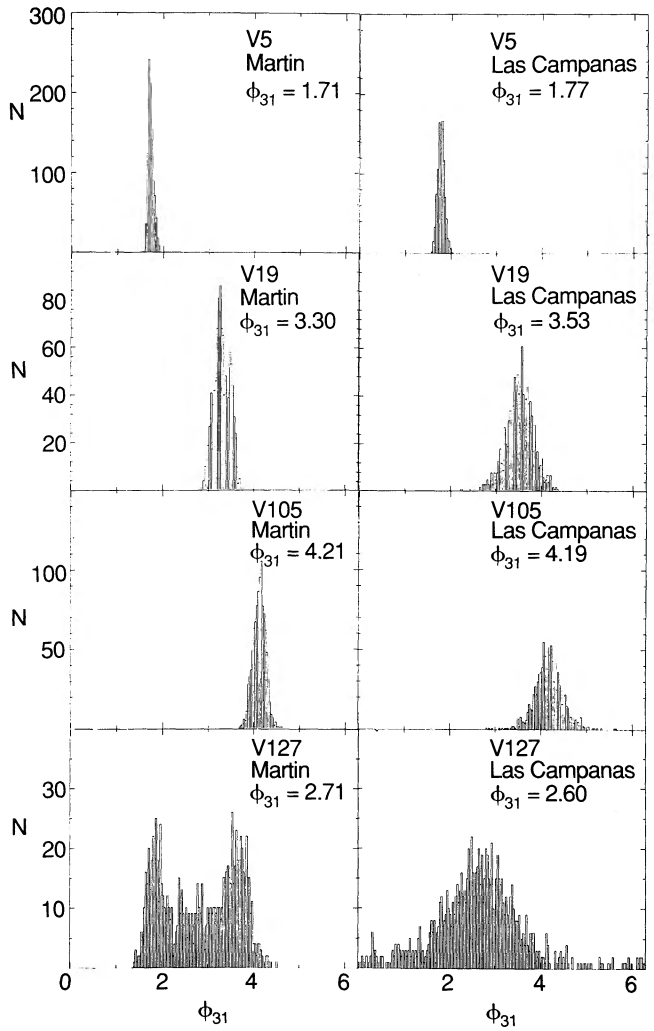

FIG. 1.—Frequency distributions of ϕ_{31} plotted for an RR*ab* star, V5, and three RR*c* stars V19, V105, and V127, in ω Centauri, for Martin's observations (*left panels*) and the Las Campanas observations (*right panels*). Each plot is based on 1000 "bootstrap" samples, and in each case the labeled value of ϕ_{31} is the value calculated from the actual observations.

value of a given phase parameter differs from the true value. Thus, for example, for V5, the ϕ_{21} half-width is 0.04 for Martin's observations and 0.06 for those of Las Campanas. In some cases, it is difficult to determine the half-width because of the cyclical nature of the phase differences. An example of this can be seen in Figure 1 for the Las Campanas observations of V127. It is difficult to assess where ϕ_{31} starts and where it ends. In this particular case, we assumed that the cycle ended (or started) at the gap in ϕ_{31} between 5.6 and 5.8. Because all of the phases have values in the range 0 to 2π, errors greater than about 2.0 in the phase parameters cannot be calculated unambiguously by the bootstrap method. What we can establish, however, is that in such cases, the errors are unacceptably large, and this is the information that we need to have.

In Table 3 we list the parameters determined from order $n = 4$ fits to the observations. These are the number of observations, period, the amplitude, the standard deviation of the fit (σ), the Fourier coefficients, A_0, A_1, the amplitude ratios R_{21}–R_{41}, ϕ_1, and the phase differences ϕ_{21}–ϕ_{41}. The "bootstrap" errors ($\sigma_{\rm Boot}$) and the standard errors calculated using Petersen's simple approximations ($\sigma_{\rm P}$) are also listed for R_{21}–R_{41} and ϕ_{21}–ϕ_{41}. The errors for Martin's data are almost all smaller than those for the Las Campanas data even though for three of the stars, the σ-values are comparable. This suggests that the ϕ_{j1} values for Martin's data are more reliable because of the larger number of observations. Another factor that seems to be important is amplitude. The large uncertainty in ϕ_{21} for V105 (Las Campanas) is caused, in part, by the small value of A_2 (or R_{21}). If the amplitude is small, it is difficult to determine a reliable value for the phase. This seems to be the reason for the large uncertainty in ϕ_{31} for V127 (Martin), as well.

One notes that the differences between Martin and Las Campanas always fall within the range of the errors estimated by both procedures, except in the case of ϕ_{21} for V19. Also, the two methods for estimating the errors give similar results. The mean values of $\sigma_{\rm Boot}$ and $\sigma_{\rm P}$ for the 24 phase differences ϕ_{j1} in Table 3 are 0.41 and 0.42, respectively, differing from each other by about 2%. The mean values for the amplitude ratios R_{j1} are $\sigma_{\rm Boot} = 0.022$ and $\sigma_{\rm P} = 0.027$ and differ by about 20%. The standard errors for the amplitude ratio, calculated by Petersen's simple calculations are, on the average, larger than those estimated by the bootstrap procedure. It is useful to test the reliability of the errors obtained by both methods using artificial data. To do this, we have simulated 20 artificial data sets in the following manner. Equation (1), along with the Fourier parameters determined for the Las Campanas observations of V105 in ω Centauri (see Table 3), was used to calculate magnitudes for the times when V105 was observed at Las Campanas. Then noise with $\sigma = 0.07$, comparable to the noise in the real data, was added to these magnitudes to generate the artificial magnitudes. These artificial magnitudes were then fitted to equation (1), and Fourier parameters were determined. The errors in the new parameters were estimated by the bootstrap procedure and by Petersen's method. The results are shown in Table 4 which gives the mean values based on the 20 simulations. Delta refers to the true error and is the difference between the parameter calculated from the simulated data and the input value (from Table 3), and $\sigma_{\rm Boot}$ and $\sigma_{\rm P}$ are the standard errors calculated by the bootstrap method and by Petersen's simple approximations, respectively. The data in Table 4 indicate that both methods give reasonable estimates of the uncertainties in the Fourier parameters. The $\sigma_{\rm P}$ values for the amplitude ratios are slightly larger than the $\sigma_{\rm Boot}$ values, as we saw in Table 3 for the real data, and it appears that the bootstrap errors are closer to the true errors. A comparison of the individual errors for the phase differences suggests that when the true errors are large (>0.5), both methods underestimate the errors, and when they are small (<0.5), both methods overestimate them. The largest discrepancy is for ϕ_{41} where both methods appear to underestimate the true error. Nevertheless, they both indicate that the errors are unacceptably large.

3.3. *The Observations of NGC 6171 and M5*

An important study of the RR Lyrae variables in NGC 6171 was that of Dickens (1970) who found that there were six RR*c* stars that were cluster members: variables 4, 6, 9, 15, 19, and 23. The star referred to here as V23 is the same as Dickens's V1. The star originally cataloged as V1 by Sawyer (1955) is a long-period variable.

Fourier parameters for the present NGC 6171 data were determined by fitting equation (1) to the observations in the same manner as was done for ω Centauri. Initially, the fits were

TABLE 3

FOURIER PARAMETERS—ω CENTAURI

Star	N	P (days)	A_B	σ	A_0	A_1	R_{21}	R_{31}	R_{41}	ϕ_1	ϕ_{21}	ϕ_{31}	ϕ_{41}
								— σ_{Boot} —				— σ_{Boot} —	
								— σ_P —				— σ_P —	
(1)	(2)	(3)	(4)	(5)	(6)	(7)	(8)	(9)	(10)	(11)	(12)	(13)	(14)
The Las Campanas Observations													
V5	157	0.5152823	1.440	0.125	15.095	0.505	0.459	0.335	0.238	5.77	3.86	1.77	5.91
							0.020	0.024	0.027		0.06	0.07	0.14
							0.031	0.029	0.029		0.08	0.12	0.16
V19	156	0.2995533	0.575	0.053	15.021	0.299	0.137	0.064	0.060	0.68	5.03	3.53	2.10
							0.017	0.019	0.023		0.17	0.28	0.31
							0.020	0.020	0.020		0.15	0.32	0.35
V105	155	0.3353345	0.618	0.072	14.950	0.311	0.026	0.074	0.023	3.21	4.54	4.19	3.40
							0.022	0.032	0.022		1.00	0.28	1.32
							0.026	0.026	0.026		0.98	0.37	1.26
V127	146	0.3052752	0.481	0.128	14.872	0.238	0.176	0.088	0.029	4.03	4.52	2.60	2.54
							0.061	0.048	0.041		0.32	0.81	1.50
							0.064	0.063	0.063		0.38	0.75	2.03
Martin's Observations													
V5	390	0.5152850	1.305	0.129	14.982	0.469	0.437	0.311	0.254	2.20	3.92	1.71	6.07
							0.015	0.013	0.014		0.04	0.06	0.07
							0.022	0.021	0.020		0.06	0.09	0.11
V19	389	0.2995525	0.524	0.060	14.937	0.270	0.130	0.100	0.059	4.47	4.62	3.30	2.41
							0.011	0.020	0.011		0.12	0.19	0.25
							0.016	0.016	0.016		0.13	0.16	0.27
V105	387	0.3353375	0.544	0.063	14.828	0.273	0.059	0.081	0.033	1.19	5.45	4.21	3.04
							0.016	0.020	0.012		0.29	0.14	0.58
							0.017	0.017	0.017		0.28	0.21	0.53
V127	401	0.3052750	0.355	0.058	14.714	0.182	0.104	0.038	0.044	1.81	4.73	2.71	0.90
							0.014	0.017	0.017		0.14	0.93	0.69
							0.022	0.022	0.022		0.22	0.56	0.51

NOTE.—Order $n = 4$.

carried out for orders $n = 4$–8, and it was found that the value of ϕ_{31} did not vary significantly for the different orders. Therefore, the Fourier parameters listed in Table 5 are for order $n = 4$. The data in this table indicate that there is a systematic increase of ϕ_{31} with period, as was found for the RR*c* stars in ω Centauri by Petersen (1984).

The most complete study of the RR Lyrae variables in M5 was done by Oosterhoff (1941). He classified 23 stars as RR*c* type. Of these, 13 could be measured on the Las Campanas plates. The Fourier parameters for the RR*c* stars that we studied in M5 were determined in the same manner as for the other clusters and are also listed in Table 5. Once again, it is apparent that the ϕ_{31} values increase with increasing period.

TABLE 4

ERRORS IN FOURIER PARAMETERS BASED ON ARTIFICIAL DATA

Parameter	$\lvert\Delta\rvert$ (mean)	σ_{Boot} (mean)	σ_P (mean)
R_{21}	0.017	0.023	0.025
R_{31}	0.024	0.024	0.025
R_{41}	0.022	0.022	0.025
ϕ_{21}	0.72	0.70	0.71
ϕ_{31}	0.43	0.46	0.46
ϕ_{41}	1.04	0.83	0.91

NOTE.—Mean errors based on 20 simulations.

The uncertainties in the ϕ_{31} values for the RR*c* stars in both NGC 6171 and M5 were estimated by Petersen's method and the bootstrap procedure. (For the bootstrap, ϕ_{31} was evaluated for 1000 samples for each star.) These errors, σ_P and σ_{Boot}, are listed in Table 6, along with the frequency distributions of ϕ_{31} for the bootstrap samples. One can readily see that both methods indicate that the values of ϕ_{31} for V9 in NGC 6171 and V78 and V80 in M5 have the largest errors. On the Las Campanas plates, the star V9 in NGC 6171 has two close companions which are not always resolved. On plates taken when the seeing in poor, V9 appears brighter than it really is, and so the light curve has excessive scatter. Thus we do not have confidence in the results for V9 in NGC 6171. The problem with V78 and V80 in M5 is different. They do not lie in crowded fields, but in both cases the amplitude A_3 is smaller than for the other stars, and this seems to be the main reason for the difficulty in determining reliable values for ϕ_{31}.

In Figure 2 we plot the ϕ_{31} values for the RR*c* stars in the three clusters against the period. The values for ω Centauri were taken from Simon (1990) and are those that Petersen (1984) determined from Martin's mean points. In this plot, we have omitted the three stars for which ϕ_{31} seems to be very uncertain (V9 in NGC 6171, and V78 and V80 in M5). The

TABLE 5

FOURIER PARAMETERS—NGC 6171 AND M5

Star	N	P (days)	A_B	σ	A_0	A_1	A_2	A_3	A_4	ϕ_1	ϕ_{21}	ϕ_{31}	ϕ_{41}
(1)	(2)	(3)	(4)	(5)	(6)	(7)	(8)	(9)	(10)	(11)	(12)	(13)	(14)
						NGC 6171							
V4	172	0.282132	0.612	0.051	15.899	0.318	0.037	0.020	0.019	4.19	5.03	3.47	2.33
V6	173	0.260256	0.649	0.065	15.905	0.334	0.049	0.025	0.021	0.94	4.83	2.38	1.66
V9	164	0.320599	0.582	0.109	15.857	0.288	0.018	0.020	0.016	6.11	5.30	4.49	1.60
V15	174	0.288589	0.620	0.064	16.010	0.321	0.030	0.032	0.019	4.67	4.46	3.55	2.20
V19	172	0.278761	0.641	0.068	16.156	0.338	0.038	0.029	0.038	0.17	4.52	3.21	1.66
V23	175	0.323343	0.611	0.057	16.061	0.302	0.027	0.023	0.022	3.64	5.03	4.11	2.67
						M5							
V15	259	0.336766	0.534	0.057	15.279	0.273	0.016	0.026	0.004	4.26	4.45	3.93	2.57
V31	246	0.300582	0.687	0.052	15.285	0.362	0.052	0.037	0.030	2.22	4.89	3.07	2.19
V35	253	0.308110	0.619	0.066	15.071	0.322	0.029	0.026	0.003	0.60	4.92	3.31	3.52
V40	257	0.317330	0.578	0.061	15.255	0.302	0.029	0.020	0.013	4.99	4.73	3.54	2.05
V44	230	0.329603	0.569	0.079	15.072	0.281	0.031	0.026	0.013	0.77	4.80	4.06	2.78
V55	256	0.328901	0.558	0.067	15.258	0.286	0.046	0.018	0.015	3.74	4.83	3.53	1.96
V62	245	0.281421	0.690	0.088	15.317	0.354	0.064	0.020	0.022	3.31	4.77	2.61	1.61
V66	251	0.350699	0.579	0.106	15.320	0.287	0.033	0.029	0.013	2.54	5.13	4.07	2.94
V73	252	0.340117	0.716	0.098	15.177	0.362	0.021	0.024	0.018	0.66	5.50	4.16	1.52
V76	236	0.432464	0.546	0.080	15.106	0.264	0.014	0.027	0.011	5.36	1.04	4.66	2.87
V78	253	0.264817	0.517	0.053	15.224	0.260	0.031	0.006	0.015	1.15	4.47	2.56	0.75
V79	254	0.333136	0.548	0.089	15.063	0.271	0.037	0.031	0.019	2.40	4.62	3.57	2.75
V80	250	0.336542	0.607	0.108	15.112	0.291	0.028	0.010	0.016	5.98	4.96	3.89	4.25

NOTE.—Order $n = 4$.

three clusters are represented by different symbols, and it is readily apparent that, in general, the NGC 6171 points lie to the left of the others in the diagram, that is, for the RR*c* stars in NGC 6171, a given value of ϕ_{31} occurs at a shorter period than in the other clusters. The points for M5 fall to the right of those for NGC 6171, mixing in with the upper envelope of the distribution of ω Centauri. Since NGC 6171 is more metal rich than M5, our results suggest that RR*c* stars are segregated in a plot of ϕ_{31} against period according to metallicity of the cluster to which they belong. A form of Hotelling's T^2 test was used to determine the significance of the difference between the two clusters. Straight lines were fitted to the data (ϕ_{31}, log P)

TABLE 6

UNCERTAINTIES IN THE ϕ_{31} VALUES FOR NGC 6171 AND M5

Star	log P	ϕ_{31}	σ_P	σ_{Boot}	Distributions of ϕ_{31} values calculated from bootstrap samples			
		(real data)			68%	90%	95%	98%
					NGC 6171			
V4	-0.550	3.47	0.28	0.29	3.26–3.84	3.10–4.01	3.03–4.11	2.98–4.19
V6	-0.585	2.38	0.29	0.23	2.13–2.59	1.97–2.77	1.87–2.85	1.79–2.97
V9	-0.494	4.49	0.61	0.49	4.00–4.98	3.64–5.49	3.24–5.77	2.66–6.04
V15	-0.540	3.55	0.22	0.17	3.35–3.69	3.23–3.80	3.18–3.90	3.12–3.97
V19	-0.555	3.21	0.25	0.22	3.05–3.48	2.91–3.64	2.82–3.70	2.77–3.79
V23	-0.490	4.11	0.27	0.30	3.78–4.38	3.57–4.50	3.46–4.55	3.32–4.62
					M5			
V15	-0.473	3.93	0.19	0.18	3.72–4.09	3.62–4.19	3.57–4.24	3.51–4.29
V31	-0.522	3.07	0.13	0.15	2.90–3.21	2.80–3.31	2.76–3.36	2.71–3.42
V35	-0.511	3.31	0.23	0.25	3.09–3.60	2.98–3.82	2.92–3.88	2.85–3.96
V40	-0.498	3.54	0.27	0.22	3.31–3.75	3.14–3.93	3.07–4.03	2.96–4.10
V44	-0.482	4.08	0.29	0.25	3.80–4.29	3.62–4.48	3.54–4.55	3.44–4.63
V55	-0.483	3.53	0.33	0.25	3.27–3.77	3.00–3.95	2.85–4.07	2.68–4.22
V62	-0.551	2.61	0.40	0.37	2.14–2.87	1.91–3.09	1.81–3.18	1.58–3.28
V66	-0.455	4.07	0.37	0.32	3.72–4.35	3.48–4.51	3.38–4.57	3.22–4.67
V73	-0.468	4.16	0.38	0.28	3.84–4.39	3.66–4.58	3.58–4.70	3.48–4.84
V76	-0 364	4.66	0.29	0.24	4.46–4.94	4.35–5.15	4.30–5.26	4.24–5.34
V78	-0.577	2.56	0.78	1.11	1.63–3.85	0.40–5.09	-0.18–5.40	-0.36–5.61
V79	-0.477	3.57	0.27	0.21	3.32–3.73	3.17–3.84	3.08–3.91	2.97–3.98
V80	-0.473	3.89	0.95	0.85	3.34–5.03	2.60–5.94	1.92–6.42	1.26–6.78

NOTE.—Order $n = 4$.

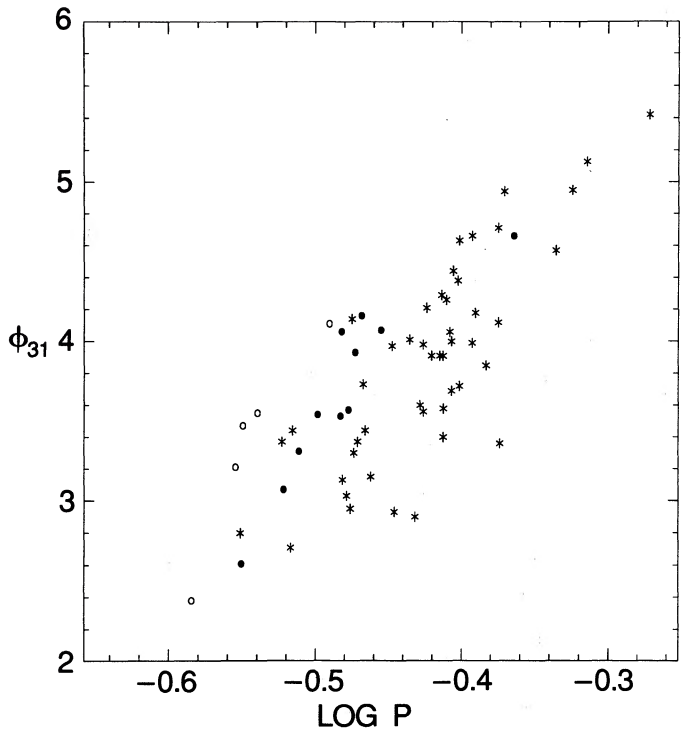

FIG. 2.—ϕ_{31} vs. log P plot for RR*c* stars in NGC 6171 (*open circles*), M5 (*solid circles*), and ω Centauri (*asterisks*).

for each cluster, and the bootstrap errors were used for weighting the ϕ_{31} values. The difference between the two clusters was found to be highly significant. (The null hypothesis, that the two lines are the same, has a 0.2% probability of being correct). This segregation, according to metal abundance, does not seem to occur among the individual stars in ω Centauri. However, it is well known that ω Centauri is an unusual cluster. Clearly it is desirable to analyze RR*c* stars in other clusters, particularly ones that are more metal poor than M5 so that the nature of the ϕ_{31}–P relation can be further explored.

4. ANALYSIS OF PUBLISHED OBSERVATIONS OF M3, M53, AND M15

Photographic observations which could be suitable for Fourier analysis have been published for RR Lyrae variables in the clusters M3, M53, and M15. These three clusters are all more metal poor than NGC 6171 and M5, with [Fe/H] values of −1.66 (M3), −2.04 (M53) and −2.17 (M15), according to Suntzeff et al. (1991).

Some 300 observations of M3 were made during the interval 1920–1926, and the magnitudes of the RR Lyrae variables were published by Larink (1922), Muller (1933), and Greenstein (1935), hereinafter referred to as LMG. These observations were analyzed by Nemec & Clement (1989) in their systematic search for double-mode RR Lyrae stars. An estimation of the light curves published by these latter authors for Larink's observations suggest that among the RR*c* stars, the data for V37, V56, V75, V85, V86, and V107 may be suitable for Fourier analysis. (The light curves for the other RR*c* stars have too much scatter.) Another major study of the RR Lyrae variables in M3 was by Szeidl (1965). His work was based on 214 plates obtained at the Konkoly Observatory from 1938 until 1962, and 17 plates taken at Hamburg in 1957. For our study, we have analyzed the magnitudes determined from the 191 Konkoly plates obtained during the interval 1950–1962, for the same six stars.

The variable stars in M53 (NGC 5024) were studied by Margoni (1964, 1965, 1967). His investigation was based on observations made with the 122 cm telescope at the Asiago Astrophysical Observatory. We include, for our analysis, the magnitudes (m_{pg}) determined for the RR*c* stars from 172 "blue" photographs taken with this telescope from 1961 to 1963.

Approximately 200 photographs of M15 were also taken with the Asiago 122 cm telescope from 1954 to 1956. The magnitudes (m_{pg}) of the RR Lyrae variables were published in a series of four papers: Mannino (1956a, b), Grubissich (1956), and Nobili (1957). We have analyzed all the RR*c* and RR*d* stars for which magnitudes were published. Fourier decomposition parameters for the RR*c* stars in M15, based on the observations of Sandage, Katem, & Sandage (1981), and those of Bingham et al. (1984) have already been determined by Kovács et al. (1986), but the parameters for the two independent data sets are not in good agreement. However, Petersen (1986) pointed out that the Fourier parameters derived from these data sets are very uncertain and concluded that more detailed observations would be required in order to determine reliable Fourier parameters. Both of these data sets contain fewer than 65 observations. Since the Asiago data, which we have used for our study, are based on 200 photographs, it is hoped that the results may prove to be more reliable.

For the variables in the clusters, M3, M53, and M15, Fourier parameters were determined from fits of order 4, except in the case of the double-mode variables in M15. (These RR*d* stars were included for completeness, even though it is not clear that the Fourier coefficients of the dominant model should be similar to those for the RR*c* stars.) The magnitudes for the RR*d* stars were fitted to the relation:

$$\text{mag} = A_0 + \sum A_j^i \cos\left[(i\omega_0 + j\omega_1)t + \phi_j^i\right], \qquad (2)$$

where the indices i and j run over all positive and negative integers, including zero, subject to the restriction

$$0 < |i| + |j| \leq n,$$
$$i + j \geq 0$$
$$j > 0 \text{ when } i + j = 0$$

(Simon 1979). In equation (2), ω_0 refers to the fundamental mode, and ω_1 refers to the first overtone. The periods P_0 and P_1 used in the calculations were those published by Clement & Walker (1991). For these RR*d* stars, the order of the fit was $n = 3$, and ϕ_{31} for the overtone mode was computed from $\phi_3^0 - 3\phi_1^0$. The Fourier parameters for the stars in these three clusters are listed in Tables 7 (M3 and M53) and 8 (M15).

The bootstrap method was used to assess the uncertainties in ϕ_{31}. The values of σ_{Boot}, based on 1000 samples for each star, are listed in column (14) of Tables 7 and 8. We used these errors to determine which values of ϕ_{31} are the most reliable. Our criterion for accepting a star was that its bootstrap error be less than 0.4. The selection of the number 0.4 was somewhat arbitrary. The idea was to exclude the stars whose ϕ_{31} values were unreliable, but, at the same time, include a reasonable number of stars in each cluster in our sample. The stars we included are variables 37, 56, 85, and 107 in M3 (LMG), vari-

TABLE 7

FOURIER PARAMETERS—M3 (NGC 5272) AND M53 (NGC 5024)

Star	N	P (days)	A_B	σ	A_0	A_1	A_2	A_3	A_4	ϕ_1	ϕ_{21}	ϕ_{31}	σ_{Boot}	ϕ_{41}
(1)	(2)	(3)	(4)	(5)	(6)	(7)	(8)	(9)	(10)	(11)	(12)	(13)	(14)	(15)
M3 - The LMG Observations														
V37	290	0.326640	0.877	0.140	15.582	0.453	0.065	0.071	0.018	2.22	4.15	2.92	0.18	2.11
V56	291	0.329600	0.775	0.127	15.513	0.422	0.053	0.043	0.027	0.46	4.42	3.14	0.22	1.41
V75	296	0.314080	0.738	0.132	15.615	0.373	0.063	0.023	0.024	3.70	4.22	3.16	0.55	1.99
V85	296	0.355824	0.843	0.133	15.405	0.440	0.041	0.061	0.001	2.33	5.04	3.77	0.16	4.66
V86	291	0.292888	0.946	0.167	15.744	0.451	0.107	0.026	0.016	4.78	4.08	2.86	0.81	2.27
V107	294	0.309034	0.917	0.146	15.503	0.465	0.068	0.034	0.016	4.01	4.59	3.47	0.35	0.49
M3 - Szeidl's Observations														
V37	178	0.3266386	0.585	0.079	15.726	0.301	0.053	0.018	0.016	0.45	4.47	2.87	0.49	1.37
V56	181	0.3295986	0.631	0.101	15.724	0.328	0.045	0.021	0.028	5.07	4.33	2.54	0.52	1.63
V75	179	0.3140762	0.597	0.102	15.675	0.300	0.040	0.038	0.022	2.35	4.89	3.02	0.28	0.45
V85	180	0.3558134	0.610	0.096	15.604	0.315	0.006	0.027	0.016	5.47	3.77	3.69	0.32	3.15
V86	174	0.2926572	0.614	0.100	15.760	0.321	0.057	0.031	0.028	1.25	4.37	3.04	0.40	1.59
V107	179	0.3090351	0.614	0.093	15.739	0.320	0.053	0.036	0.026	5.85	4.21	2.67	0.29	1.78
M53 - The Asiago Observations														
V2	128	0.38614325	0.509	0.075	16.627	0.263	0.020	0.016	0.016	4.54	4.78	3.52	0.64	2.49
V4	143	0.38565475	0.434	0.081	16.600	0.223	0.017	0.015	0.008	3.36	0.58	3.04	0.61	1.08
V15	146	0.30871070	0.411	0.088	16.584	0.207	0.007	0.019	0.014	4.39	2.28	2.07	0.59	0.83
V16	141	0.30317625	0.392	0.093	16.623	0.166	0.036	0.026	0.007	3.08	4.97	0.61	0.56	0.67
V17	135	0.38120450	0.477	0.086	16.572	0.241	0.010	0.006	0.008	2.74	0.38	2.23	1.48	4.04
V19	143	0.39137825	0.478	0.110	16.597	0.237	0.031	0.040	0.020	5.94	0.66	3.70	0.29	4.74
V20	147	0.38425175	0.403	0.079	16.605	0.208	0.015	0.008	0.011	4.83	4.24	3.02	1.06	2.20
V21	146	0.33851350	0.598	0.088	16.611	0.276	0.077	0.048	0.022	2.47	4.01	2.80	0.23	1.11
V23	143	0.36565350	0.581	0.115	16.620	0.268	0.070	0.053	0.017	0.05	5.79	3.69	0.37	0.19
V26	136	0.39111660	0.496	0.079	16.547	0.233	0.019	0.027	0.032	3.91	4.11	4.70	0.42	1.52
V32	151	0.39036900	0.387	0.102	16.544	0.196	0.026	0.008	0.003	5.54	5.41	3.15	1.17	0.80
V35	133	0.37267390	0.472	0.100	16.633	0.192	0.029	0.036	0.037	1.33	4.74	4.47	0.35	4.37
V36	143	0.37316850	0.459	0.080	16.566	0.237	0.022	0.015	0.011	4.28	6.10	3.22	0.32	4.55
V40	134	0.31480760	0.653	0.141	16.762	0.348	0.018	0.061	0.009	3.26	5.21	2.81	0.25	0.47
V47	145	0.35049700	0.597	0.083	16.493	0.322	0.012	0.043	0.011	5.81	5.12	3.31	0.19	3.86

NOTES.—Order $n = 4$. σ_{Boot} refers to the error in ϕ_{31}.

TABLE 8

FOURIER PARAMETERS—M15 (NGC 7078)

Star	N	P (days)	A_B	σ	A_0	A_1	A_2	A_3	A_4	ϕ_1	ϕ_{21}	ϕ_{31}	σ_{Boot}	ϕ_{41}
(1)	(2)	(3)	(4)	(5)	(6)	(7)	(8)	(9)	(10)	(11)	(12)	(13)	(14)	(15)
V3	200	0.38873700	0.638	0.101	15.919	0.323	0.066	0.031	0.021	4.33	3.88	3.28	0.33	1.55
V4	198	0.31357180	0.806	0.100	15.943	0.363	0.117	0.029	0.017	6.08	3.98	1.56	0.37	5.95
V5	197	0.38420625	0.673	0.091	15.867	0.326	0.076	0.025	0.006	1.73	4.00	1.71	0.37	1.20
V7	106	0.36758100	0.632	0.157	15.872	0.286	0.076	0.060	0.036	0.77	4.89	2.60	0.43	1.49
V10	184	0.38639425	0.649	0.109	15.974	0.305	0.066	0.056	0.017	5.24	4.57	2.84	0.21	2.68
V11	198	0.34325000	0.662	0.145	15.955	0.318	0.079	0.020	0.043	1.39	3.83	5.07	0.70	0.99
V14	198	0.38198575	0.534	0.084	16.042	0.263	0.053	0.022	0.016	3.20	3.94	1.78	0.40	2.24
V17	180	0.42889600	0.551	0.096	15.910	0.333	0.088	0.053	-	4.71	4.33	2.40	0.28	-
V18	182	0.36769125	0.698	0.114	15.943	0.352	0.091	0.021	0.033	6.05	3.74	2.58	0.56	0.36
V24	140	0.36967250	0.822	0.110	15.972	0.375	0.102	0.066	0.007	3.75	3.97	2.81	0.21	5.01
V26	188	0.40227200	0.586	0.091	16.011	0.280	0.048	0.026	-	5.98	5.23	3.37	0.54	-
V30	189	0.40598600	0.599	0.093	15.709	0.244	0.037	0.027	-	5.07	5.28	3.18	0.52	-
V31	184	0.40817400	0.550	0.074	16.037	0.221	0.033	0.042	-	0.62	4.31	3.48	0.24	-
V35	194	0.38402625	0.567	0.109	16.097	0.293	0.038	0.027	0.007	0.49	3.76	2.89	0.35	5.39
V38	194	0.37527750	0.741	0.101	15.925	0.361	0.035	0.023	0.027	2.13	4.52	2.85	0.39	3.68
V39	188	0.38957400	0.610	0.089	15.975	0.300	0.033	0.016	-	0.45	3.83	3.67	1.02	-
V40	184	0.37731400	0.723	0.103	15.932	0.350	0.044	0.027	0.028	2.64	4.67	2.76	0.41	3.41
V42	195	0.36017460	0.747	0.084	15.875	0.366	0.057	0.026	0.027	2.95	4.65	2.46	0.43	0.59
V43	191	0.39597375	0.665	0.071	15.981	0.355	0.041	0.049	0.015	4.28	4.88	3.26	0.14	1.54
V50	126	0.29806225	0.551	0.084	15.867	0.260	0.059	0.015	0.019	4.11	3.39	0.59	0.70	1.05
V51	115	0.39695200	0.310	0.062	15.819	0.143	0.021	0.022	-	5.27	6.18	2.59	0.56	-
V53	192	0.41413400	0.612	0.117	15.889	0.269	0.000	0.021	-	3.65	5.49	1.97	0.51	-
V54	114	0.39957410	0.236	0.054	15.806	0.107	0.010	0.025	0.015	5.49	2.92	2.05	0.37	0.74
V66	186	0.37934400	0.424	0.096	16.035	0.211	0.039	0.025	0.010	4.97	4.35	2.80	0.45	0.28
V99	199	0.27993500	0.350	0.104	15.923	0.176	0.015	0.022	0.002	4.84	4.61	2.19	0.45	2.45

NOTES.—Order $n = 4$ for the RR*c* stars. Order $n = 3$ for the RR*d* stars. σ_{Boot} refers to the error in ϕ_{31}.

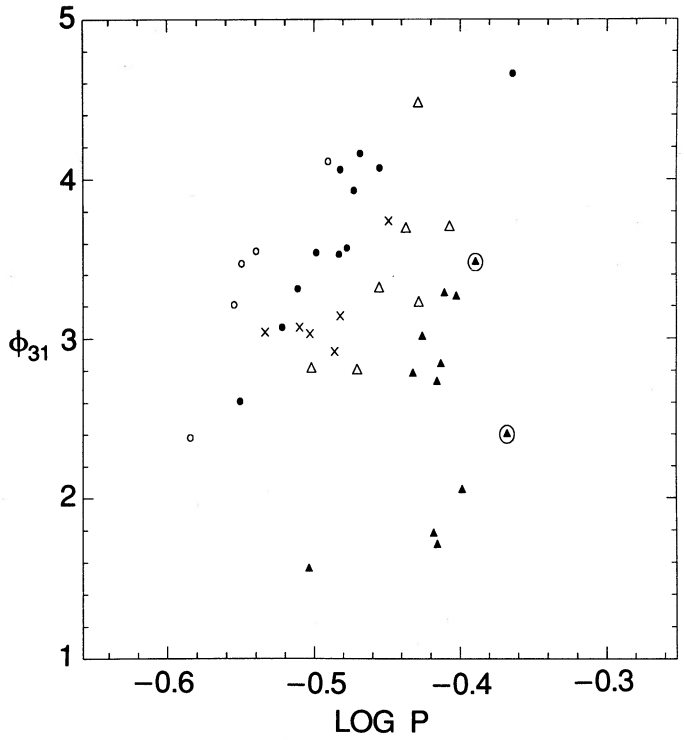

FIG. 3.—ϕ_{31} vs. log P plot for RRc stars in NGC 6171 (*open circles*), M5 (*solid circles*), M3 (*crosses*), M53 (*open triangles*), and M15 (*solid triangles*). The RRd stars in M15 are represented by solid triangles enclosed in circles. The metallicities, [Fe/H], of these five clusters are −0.99, −1.40, −1.66, −2.04, and −2.17, for NGC 6171, M5, M3, M53, and M15, respectively. The stars plotted all have errors (σ_{Boot}) in ϕ_{31} of less than 0.4.

ables 75, 85, 86, and 107 in M3 (Szeidl), variables 19, 21, 23, 35, 36, 40, and 47 in M53, and variables 3, 4, 5, 10, 14, 17, 24, 31, 35, 38, 43, and 54 in M15.

Figure 3 is a plot of ϕ_{31} versus period for these stars, with each cluster represented by a different symbol. For the two stars in M3 (V85 and V107) for which both the LMG data and Szeidl's have been included, we have plotted the mean value of ϕ_{31}. Also included in the diagram are the data for NGC 6171 and M5. In Figure 3 one sees that for each cluster, there seems to be a systematic increase of ϕ_{31} with period, although there is considerable scatter. We note that most of the M3 points are shifted to the right of those for M5, and to the left of those for M53, while those for M53 lie to the left of those for M15. Thus, in a plot of ϕ_{31} against period, the RRc stars in NGC 6171, M5, M3, M53, and M15 appear to be ranked according to metal abundance.

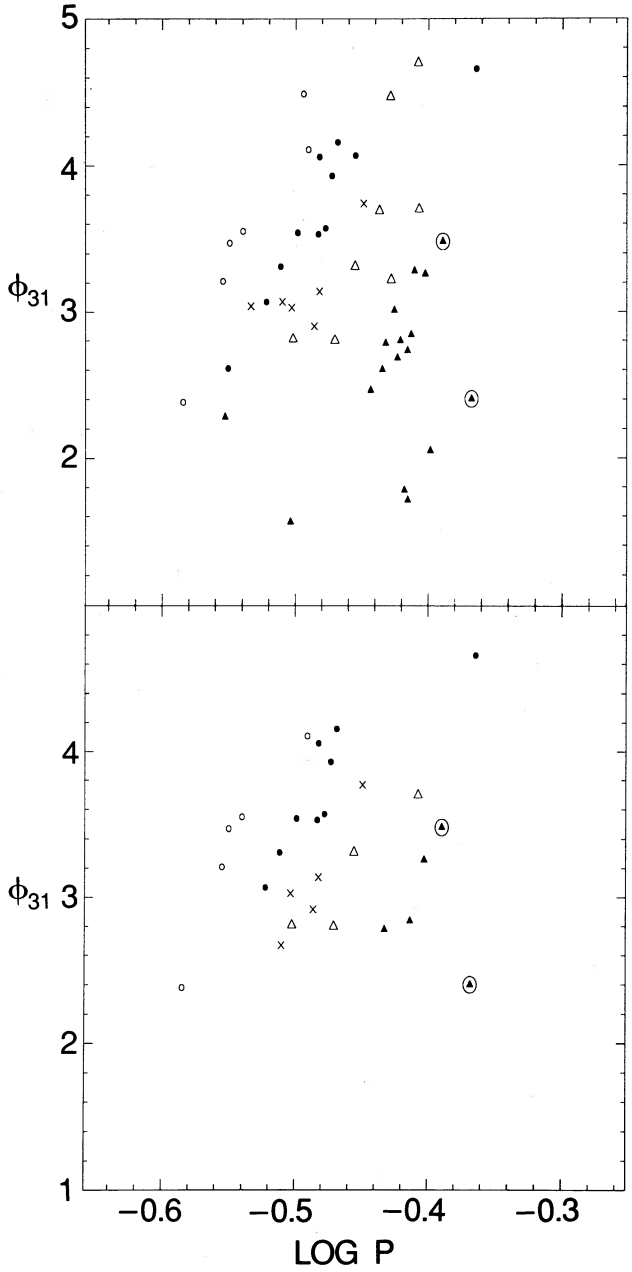

FIG. 4.—ϕ_{31} vs. log P plot for the same five clusters as in Fig. 3. The symbols are the same as in Fig. 3. The stars plotted in the upper panel of the diagram are those with errors, σ_{Boot}, less than 0.5; those in the lower panel have errors less than 0.3.

5. DISCUSSION

It has already been noted that our criterion for accepting stars to be plotted in Figure 3 was arbitrary. This criterion required that the bootstrap errors be less than 0.4. In Figure 4 we show two further ϕ_{31}–period plots in which the acceptable error is (1) increased to 0.5, and (2) decreased to 0.3. In the former case (top panel of Fig. 4), seven stars are added, three of which scatter off the metallicity segregation seen in Figure 3. Nonetheless, this segregation is generally preserved. In the bottom panel of Figure 4, the strengthened criterion results in the deletion of many stars. The result is a tightening of the metallicity segregation—exactly what one would expect if the effect is real. Perhaps most interesting is that the splitting of the M15 sequence, seen in Figure 3 and the upper panel of Figure 4, virtually disappears in the bottom panel of Figure 4. This hints that the lower sequence might be an artifact caused by the uncertainties in the observations.

In the opinion of the present authors, Figures 3 and 4 constitute strong evidence that (1) the RRc stars in a given globular cluster show a sequence of ϕ_{31} increasing with period, and (2) the larger the cluster metallicity, the higher the sequence lies on the ϕ_{31}–period plot. Thus a clear progression is seen with metallicity, such that a decrease in [Fe/H] mandates a longer

period for fixed value of ϕ_{31}. Whereas quantification of the Sandage period-shift effect depends on measuring or inferring the temperature in some way, the progression demonstrated in the present work appears in terms of ϕ_{31}, a quantity which can be straightforwardly determined to any desired accuracy provided the observational data are precise enough. Future CCD observations of RR*c* stars in globular clusters will be useful to establish the relationship among ϕ_{31}, period, and metallicity with greater precision.

What is the physical significance of the ϕ_{31}–period diagram? Using observational data from ω Centauri, Simon (1989, 1990) interpreted the spread in period at fixed ϕ_{31} as a mass effect, with the mass increasing with rising period. However, the ω Centauri masses, thus inferred, showed no correlation with metallicity. If the present ϕ_{31} period plot also bespeaks a mass effect, then an inverse relationship between mass and metallicity is inferred in globular clusters containing RR*c* stars. Indeed, this was the prediction made by Simon 1989 (namely, the larger [Fe/H] implies a higher locus in the diagram) and confirmed in the present investigation.

However, the results in ω Centauri depended upon pulsation models which employed standard (Los Alamos) opacities. Since the new Opal opacities (Iglesias & Rogers 1991) are known to exhibit strong metallicity effects (Kovács et al. 1991), it is not clear how much, if any, of the metallicity segregation on the ϕ_{31}–period diagram is due to opacity rather than mass. This will need to be tested with new hydrodynamic models. At the same time, the HB evolutionary tracks must be recalculated with new opacities, and cluster metallicities measured with improved accuracy to allow precise determinations of the RR*d* mass. Thus a great deal of work remains before the RR Lyrae stars can be made to yield their luminosities and masses.

We would like to thank Donald Fernie and Slavek Rucinski for useful comments during the preparation of this paper. Thanks are also due to Michael Evans of the Department of Statistics at the University of Toronto for performing the statistical test discussed in § 3.3. N. R. S. is pleased to acknowledge support for this work under the NASA Astrophysics Theory Program, grant NAGW-2395. C. Clement is grateful for support from the Natural Sciences and Engineering Research Council of Canada.

REFERENCES

Bingham, E. A., Cacciari, C., Dickens, R. J., & Fusi-Pecci, F. 1984, MNRAS, 209, 765
Clement, C. M., & Walker, I. 1990, AJ, 101, 1352
Cox, A. N. 1991, ApJ, 381, L71
Diaconis, P., & Efron, B. 1983, Sci. Am., 248, No. 5, 116
Dickens, R. J. 1970, ApJS, 22, 249
Greenstein, J. L. 1935, Astron. Nach., 257, 301
Grubissich, C. 1956, Contr. Padova-Asiago, No. 76
Iglesias, C. A., & Rogers, F. J. 1991, ApJ, 371, L73
Kovács, G., Buchler, J. R., & Marom, A. 1991, A&A, 252, L27
Kovács, G., Shlosman, I., & Buchler, J. R. 1986, ApJ, 307, 593
Larink, J. 1922, ABergedorf, 2, No. 6
Lee, Y.-W., Demarque, P., & Zinn, R. 1990, ApJ, 350, 155
Mannino, G. 1956a, Contr. Padova-Asiago, No. 74
Mannino, G. 1956b, Contr. Padova-Asiago, No. 75
Margoni, R. 1964, Contr. Padova-Asiago, No. 150
Margoni, R. 1965, Contr. Padova-Asiago, No. 170
Margoni, R. 1967, Contr. Padova-Asiago, No. 198
Martin, W. C. 1938, Leiden Ann., 17, pt 2
Muller, Th. 1933, Veroff. Berlin-Babels., 11, 1
Nemec, J. M., & Clement, C. M. 1989, AJ, 98, 860
Nobili, F. 1957, Contr. Padova-Asiago, No. 81
Oosterhoff, P. Th. 1941, Leiden Ann., 17, pt 4
Petersen, J. O. 1984, A&A, 139, 496
Petersen, J. P. 1986, A&A, 170, 59
Rood, R. T. 1990, in Confrontation between Stellar Pulsation and Evolution, ed. C. Cacciari & G. Clementini (San Francisco: ASP), 11
Sandage, A. 1982, ApJ, 350, 631
Sandage, A., Katem, B., & Sandage, M. 1981, ApJS, 46, 41
Sawyer, H. B. 1955, Publ. David Dunlap Obs. 2, No. 2
Seares, J. H., Kapteyn, J. C., & Rhijn, P. J. 1930, Mt. Wilson Catalogue of Photographic Magnitudes in Selected Areas 1–139, Mt. Wilson Obs. Papers, Vol. 4
Simon, N. R. 1979, A&A, 74, 30
Simon, N. R. 1988, in Pulsation and Mass Loss in Stars, ed. R. Stalio & L. A. Willson (Dordrecht: Reidel), 27
Simon, N. R. 1989, ApJ, 343, L17
Simon, N. R. 1990, ApJ, 360, 119
Simon, N. R. 1992, ApJ, 387, 162
Simpson, G., & Mayer-Hasselwander, H. 1986, A&A, 162, 340
Stellingwerf, R. F. 1978, ApJ, 224, 953
Stellingwerf, R. F., & Dickens, R. J. 1987, ApJ, 322, 133
Suntzeff, N. B., Kinman, T. D., & Kraft, R. P. 1991, ApJ, 367, 528
Szeidl, B. 1965, Budapest Mitt., No. 58
Woolley, R. v. d. R. 1966, R. Obs. Ann., No. 2